

# RadEye: Tracking Eye Motion Using FMCW Radar

Shichen Zhang  
Computer Science and Engineering  
Michigan State University  
East Lansing, Michigan, USA  
sczhang@msu.edu

Qijun Wang  
Computer Science and Engineering  
Michigan State University  
East Lansing, Michigan, USA  
qjwang@msu.edu

Kunzhe Song  
Computer Science and Engineering  
Michigan State University  
East Lansing, Michigan, USA  
songkunz@msu.edu

Qiben Yan  
Computer Science and Engineering  
Michigan State University  
East Lansing, Michigan, USA  
qyan@msu.edu

Huacheng Zeng  
Computer Science and Engineering  
Michigan State University  
East Lansing, Michigan, USA  
hzeng@msu.edu

## Abstract

Eye motion tracking plays a vital role in many applications such as human-computer interaction (HCI), virtual reality, and disease detection. Camera-based eye tracking, albeit accurate and easy to use, may raise privacy concerns and appear to be unreliable in poor lighting conditions. In this paper, we present RadEye, a radar system capable of detecting fine-grained human eye motions from a distance. RadEye is realized through an integrated hardware and software design. It customizes a sub-6GHz FMCW radar so as to detect millimeter-level eye movement while extending its detection range using low frequency. It further employs a deep neural network (DNN) to refine the detection accuracy through camera-guided supervisory training. We have built a prototype of RadEye. Extensive experimental results show that it achieves 90% accuracy when detecting human eye rotation directions (up, down, left, and right) in various scenarios.

## CCS Concepts

• **Human-centered computing** → **Human computer interaction (HCI)**; • **Hardware** → Printed circuit boards.

## Keywords

FMCW radar, Human-Computer Interaction, Eye tracking, Deep learning

### ACM Reference Format:

Shichen Zhang, Qijun Wang, Kunzhe Song, Qiben Yan, and Huacheng Zeng. 2025. RadEye: Tracking Eye Motion Using FMCW Radar. In *CHI Conference on Human Factors in Computing Systems (CHI '25)*, April 26–May 01, 2025, Yokohama, Japan. ACM, New York, NY, USA, 13 pages. <https://doi.org/10.1145/3706598.3713775>

## 1 Introduction

Eye motion tracking has many applications. As per the Amyotrophic Lateral Sclerosis (ALS) Association, more than 5,000 people in the U.S. are diagnosed with ALS every year [1]. Individuals with ALS

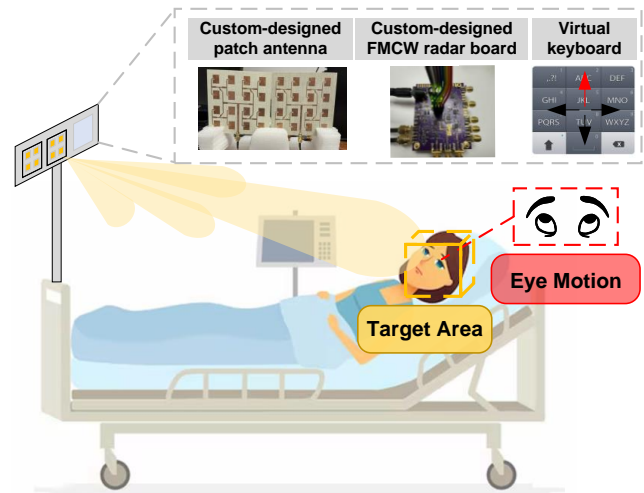


Figure 1: Illustration of RadEye.

lose control of their muscles and thus cannot move, speak, eat, and breathe [28]. Eye movements become their only method to convey messages for communications [2]. A non-intrusive, privacy-preserving eye tracking system can better understand their conveying messages and help them achieve efficient communications. In addition to assisting individuals with disabilities, eye motion tracking can serve as an effective human-computer interaction (HCI) tool in various scenarios. For example, it can help immobile patients communicate, as illustrated in Fig. 1. It can also be used to remotely control devices such as smart TVs, home appliances, elevators, and virtual reality systems. Furthermore, a reliable eye-tracking system has broader applications in healthcare, including psychology research [25], marketing analysis [44], and early disease detection [31].

Existing contactless eye tracking solutions employ various sensors, including cameras, acoustic, and radar. While cameras have demonstrated high accuracy in eye motion detection [10, 33], their application may pose privacy concerns in some scenarios. Additionally, cameras do not perform well in poor lighting conditions. Recently, acoustic signals have been studied for eye tracking on smartphones [5, 22]. However, due to the propagation nature of sounds, acoustic-based eye tracking systems are limited to eye blink



This work is licensed under a Creative Commons Attribution 4.0 International License. *CHI '25, Yokohama, Japan*  
© 2025 Copyright held by the owner/author(s).  
ACM ISBN 979-8-4007-1394-1/25/04  
<https://doi.org/10.1145/3706598.3713775>

detection within a small distance. Millimeter-wave (mmWave) radio frequency (RF) radar has also been studied for facial recognition and eye blink detection (e.g., [13, 46]). While mmWave radar can achieve mm-level motion detection, its detection range is very limited due to its small wavelength. Additionally, existing mmWave-based sensing work focuses mainly on eye blink detection rather than eye motion tracking. Low-frequency radio signals have been widely leveraged for fine-grained human activity recognition (HAR), such as Wi-Fi sensing [9, 15, 19, 20, 36, 37], RFID sensing [35, 43], and 4G/5G sensing [7, 40]. However, due to their large wavelength as well as their non-coherent sensing approaches, those systems may not be able to detect such subtle eye motions. So far, there is no RF-based system that can track human eye motions from a distance.

In this paper, we present RadEye, an RF sensing system that can track eye motions from a distance. Compared to camera-based eye tracking, RadEye not only mitigates privacy concerns but also performs reliably in poor lighting conditions. The privacy-preserving nature of RF signals stems from their inherent characteristics. Unlike camera images, RF signals are not visually interpretable by humans and inherently possess low spatial resolution. As a result, they are unlikely to reveal detailed, identifiable features of individuals. Extracting personal information from RF signals involves complex processes that require advanced signal processing and AI models, making misuse significantly less accessible compared to camera systems. Furthermore, RF sensing systems are typically designed to capture only coarse-grained human activities—such as presence, movement, or positioning—rather than detailed personal characteristics like facial features or voice. This makes RF-based sensing systems inherently more privacy-preserving than cameras, ensuring better protection of individual privacy.

Compared to acoustic- and mmWave-based eye detection approaches, RadEye extends both the RF sensing capability (from eye blink to eye motion) and detection range (from less than 1 m to more than 5 m). We note that the eye motion tracking task is very different from eye blink detection. The former is a regression problem, while the latter is a binary classification problem. Such an extension will significantly enlarge RadEye’s application landscape in real life.

In the design of RadEye, we face two challenges. **Challenge #1: subtle eye movement and long detection range.** On one hand, eye rotation, encompassing eyelid and eye muscle displacement, involves movement around 1 mm [18]. Such a subtle motion makes it hard to detect for an RF system. On the other hand, an eye-tracking sensor may be used in indoor or outdoor scenarios. The eye detection distance varies significantly, ranging from 0.5 m (e.g., from smartphone to eyes) to 5 m (e.g., from smart TV to eyes). Devising an RF system that can detect subtle (mm-level) eyeball rotation movement from a distance is not a trivial task. **Challenge #2: interference mitigation by design.** An eye-tracking system may suffer from interference from three sources: i) multipath from the target person to the RF sensor, ii) the movement of the target person’s other body parts such as chest breathing, arm waving, and leg shaking, and iii) other moving objects/people in the area. For instance, when the RF sensor detects eye movement, another person may walk around in the same room, generating interference to the received signals at the RF sensor. In general, interference is a notorious problem for RF sensing. Given the subtlety of eyeball

**Table 1: Comparison of RadEye and existing eye detection works.**

Reference	Technique	Max. distance	Track eye motion	Work in low light
Blink Listener [22]	Acoustic	0.8 m	✗	✓
TwinkleTwinkle [5]	Acoustic	0.6 m	✗	✓
BlinkRadar [13]	IR-UWB	0.8 m	✗	✓
X. Zhang [47]	mmWave	1.2 m	✗	✓
C. Ryan [27]	Event Camera	0.6 m	✓	✗
GazeRecorder [10]	Web Camera	0.7 m	✓	✗
<b>RadEye</b>	Sub-6GHz FMCW Radar	5 m	✓	✓

movement, the interference must be mitigated by design so as to accurately detect eye’s movement.

RadEye addresses the above two challenges through a joint hardware and software design. To achieve the required detection resolution and range (i.e., Challenge #1), we design and optimize a 5 GHz FMCW radar for eye movement tracking. We choose 5 GHz radar for two reasons: i) high-frequency radio wave (e.g., mmWave) is suited for detecting tiny motions, but has a small detection range; and ii) low-frequency radio wave is suited for long detection, but not suited for detecting subtle movement. A tradeoff between detection resolution and range leads to our selection of 5 GHz frequency band. Additionally, the market has rich electronic devices (e.g., power amplifiers, mixers, and low noise amplifiers) at 5 GHz frequency bands due to the maturity of Wi-Fi industry. Thus, it is cost-friendly to build 5 GHz radars. To mitigate interference from multipath and other moving objects (i.e., Challenge #2), we combine four techniques: i) FMCW modulation for the 5 GHz radar, ii) a sophisticated signal processing pipeline for eye-related feature extraction, iii) a transformer-based deep neural network (DNN) for eye motion detection, and iv) a camera-guided supervisory training method for the DNN model. Together, these four techniques make RadEye capable of separating the eye motion features from the interference from multipath and other objects. More importantly, these four techniques make RadEye transferable to unseen scenarios, enhancing its generalizability in practice.

We have built a prototype of RadEye and evaluated its performance in multiple scenarios. Experimental results show that, for a person at a 5 m distance, the average estimation error of eye rotation is 24 degrees in azimuth and 21 degrees in elevation. By formulating the eye rotation problem to a classification (up, down, left, and right) problem, RadEye achieves 90% accuracy. Extensive results confirm the generalizability of RadEye in unseen scenarios as well as its resilience to interference.

Table 1 shows how RadEye advances the state-of-the-art (SOTA) RF sensing technology. The main contributions of RadEye are summarized as follows:

- To the best of our knowledge, RadEye is the first-of-its-kind system that utilizes RF signals to estimate eye rotation angles from a distance.
- RadEye presents a joint hardware and software scheme for subtle eye motion detection in the presence of interference.
- Extensive experimental results validate the performance, robustness, and generalizability of RadEye.

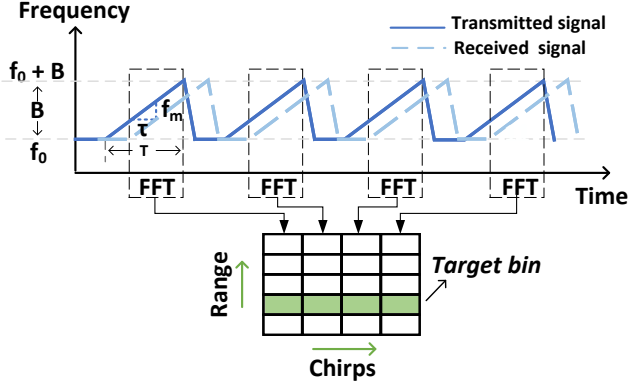


Figure 2: Illustration of FMCW signal.

## 2 RadEye: Design Analysis

### 2.1 Background

RadEye leverages the FMCW signal to detect the eye motions. The signal is transmitted from the radar's TX antenna towards the eyes; and the reflective signal from the eyes is received by the radar's RX antenna. The difference between the transmitted and received signal is used to extract the eye motion features. As shown in Fig. 2, the FMCW signal starts from frequency  $f_0$  and ramps up linearly over time  $T$ . The transmitted signal can be written as:

$$S_T(t) = e^{-j2\pi(f_0 t + \frac{B}{2T} t^2)}. \quad (1)$$

The received signal reflected from the target can be written as:

$$S_R(t) = \alpha e^{-j2\pi(f_0(t-\tau) + \frac{B}{2T}(t-\tau)^2)}. \quad (2)$$

The transmitted and received signals are mixed together, leading to an immediate frequency (IF) signal as follows:

$$S_M(t) = S_T(t)S_R(t)^* = \alpha e^{-j2\pi(f_0 \tau + \frac{B}{T} \tau t - \frac{B}{2T} \tau^2)}. \quad (3)$$

RadEye uses the IF signal to infer the eye motions. As we can see from the Eqn. 3, both the frequency and phase of the IF signal are proportional to the delay of the signal. The frequency of the IF signal  $f_m = \frac{B}{T} \tau$ . The time delay can be calculated as  $\tau = \frac{f_m T}{B}$  and, as a result, the distance can be calculated by  $d = \frac{c\tau}{2} = \frac{c f_m T}{2B}$ .

To separate the signal reflected from different objects, we do range-FFT on each chirp of the IF signal, as illustrated in Fig. 2. Each range bin represents the signal coming from different distances. The range resolution  $\Delta d = \frac{c}{2B}$  is determined only by the bandwidth of the signal. To identify the FFT bin corresponding to eye motions, a user will be asked to blink his/her eye as a reference. The algorithm will be presented in §3.

### 2.2 Detectability of Human Eye Rotation

The kinematics of eye rotation is a complex process involving the stretching and contraction of six extraocular muscles. The combined movement of these muscles alters the shape of the reflection surface, affecting the length of the signal reflection path and influencing the phase shift of the FMCW signal. Additionally, these muscle movements impact signal attenuation, as muscles and surrounding tissues absorb and scatter FMCW signals to varying degrees based

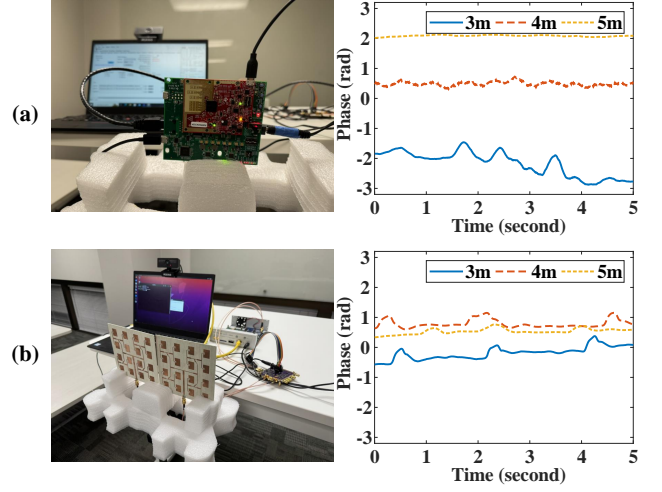


Figure 3: (a) The phase change of the corresponding FFT-bin from the mmWave radar. (b) The phase change of the corresponding FFT-bin from the RadEye.

on their density, composition, and position. When eye muscles move, the spatial distribution of these tissues changes, altering the amount of signal absorbed or scattered and leading to variations in attenuation.

In addition to muscle movements, eyelid motion also affects reflected FMCW signals. During eye rotations, the eyelids fold or stretch, and this change in thickness modifies the distance of the signal reflection path. Furthermore, eyelid movement alters the size of the exposed area of the eyeball, further influencing the attenuation of the reflected signal.

### 2.3 Feasibility Analysis

We conducted experiments to compare the performance of RadEye with a 60 GHz FMCW mmWave radar (i.e., AWR6843 [32]), both of which have 1.1 GHz bandwidth. Specifically, a participant performed eye blinks at distances of 3 m, 4 m, and 5 m. Fig. 3 presents our experimental measurements. The experimental results show that mmWave radar can detect human eye blinks within a range of 3 meters. However, the detectability decreases rapidly as the distance increases. In contrast, RadEye exhibits a consistent capability of detecting human eye blinks at those three distances.

In some cases, the line-of-sight path from human eyes to the radar device might be blocked. Thus, we conducted comparative tests to evaluate the ability of two types of radars to track eye movements under obstructed conditions. To simulate such cases, we repeated the same test at a distance of 3 m but placed a wooden door between the radar and the participant. As shown in Fig. 4, RadEye is capable of detecting eye blinks even behind the door, whereas the mmWave radar fails to do so. This limitation of the mmWave radar can likely be attributed to the high attenuation of mmWave signals. It is worth noting that these experiments were conducted in the same environment and used an identical signal processing pipeline. The detailed parameters of the two systems are provided in Table 2.

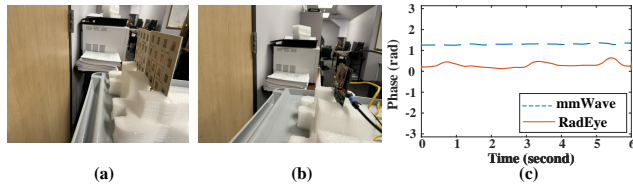


Figure 4: (a) RadEye tracking behind a wooden door. (b) mmWave radar tracking behind a wooden door. (c) Phase change of the corresponding FFT-bin from both systems.

Table 2: Detailed Parameters for the RadEye and mmWave Radar.

Parameters	Systems	
	RadEye	AWR6843
Tx / Rx antenna gain	15 dBi	7 dBi
Transmission power	15 dBm	12 dBm
Chirp duration	600 $\mu$ s	600 $\mu$ s
Idle time	400 $\mu$ s	400 $\mu$ s
Bandwidth	1.1 GHz	1.1 GHz
Gain figure (Rx chain)	–	48 dB
Noise figure (Rx chain)	7 dB	12 dB
Gain from baseband amplifier	8 dB	–

**Millimeter-Level Motion Detection.** As we mentioned earlier, the ranging resolution of an FMCW radar is not enough to detect the tiny eye motion. However, the phase of the demodulated FMCW signal can reflect the eye rotation motion. Eye rotation involves eyelid and eye muscles displacement, which moves at millimeter level [18]. Based on Eqn. (3), one-millimeter movement of eyeball can cause a phase change of FMCW signal by:  $2\pi f_0 \frac{2d}{c} = 0.25$  radian (i.e.,  $14^\circ$ ), which is easy to detect and measure on the corresponding Range-FFT bin.

**Resilience to Interference.** An eye-tracking system may suffer from interference from three sources: i) multipath from the target person to the RF sensor, ii) the movement of the target person's other body parts such as chest breathing, arm waving, and leg shaking, and iii) other moving objects/people in the area. To mitigate such interference, RadEye employs wideband FMCW modulation and high-optimized directional antennas. The FMCW modulation with 1.1 GHz offers a ranging resolution of 14 cm, allowing RadEye to distinguish objects separated by 14 cm. The FMCW modulation can effectively filter out the interference from the target person's other body motions such as chest breathing. A custom-designed patch antenna is used for signal transmission and reception, serving as an angular filter for suppressing interference from other directions. As shown in Fig. 5, the patch antenna has a 3 dB beamwidth of 21 degrees. In addition to the hardware design and optimization, a transformer-based DNN, trained through a video-guided pipeline, will be useful to focus on the desired features while eliminating the interfering features through a self-attention mechanism.

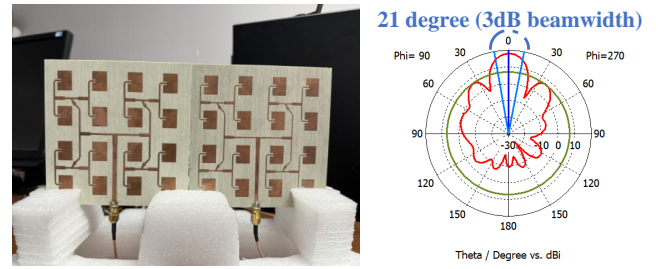


Figure 5: The custom-designed patch antennas (left) and their gain pattern (right).

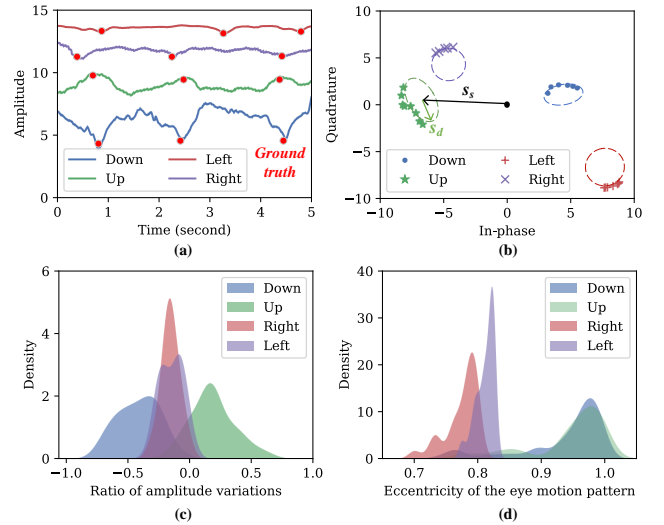


Figure 6: The feature for eye rotations. (a) The signal amplitude when eye rotates toward different directions. (b) The signal in the complex domain when eye is rotating. (c) The kernel density estimation of the signal amplitude variation ratio. (d) The kernel density estimation of the motion pattern eccentricity.

## 2.4 Feature Validation

We conducted a preliminary study of the sub-6GHz radar's capability for detecting eye motions. A participant was seated 3 m in front of the radar and instructed to rotate his eyeballs in four different directions (up, down, left, and right). Fig. 6(a) depicts the signal amplitude from the corresponding Range-FFT bin during these eye rotations. The "Ground truth" points in the figure were captured by a camera with the SOTA computer vision-based eye detection algorithm [17], marking the moment of real eye rotations. It is evident that the eyeball rotations towards the four directions indeed induce the amplitude change of the radar's IF signal. This indicates that the 5 GHz FMCW radar is capable of capturing the eye motions. When delving into eye rotation signals in different directions, we observe that up/down movements exhibit a more substantial change compared to left/right movements. This is not surprising, because the eyelid of vertical actions has larger movements. Additionally, the up-rolling of eyes results in an amplitude increase. This is because the eyelid's movement during the upward gaze involves more parts

of the eyeball in reflection. The water-textured nature of the eyeball, in contrast to the skin, enhances signal reflection. Given that the different eye rotations cause different amplitude changes, we use the amplitude variation ratio as one of the features for inference.

**Features in Complex Domain.** In addition to the observation in the temporal domain, we further observe the IF signal in the complex domain as shown in Fig. 6(b). For the eye motion signal  $S_e$  from the corresponding Range-FFT Bin, it can be decomposed into a static component  $S_s$  and a dynamic component  $S_d$ . They can be written as:

$$S_e = S_d + S_s = \alpha_d e^{j\phi_d} + \alpha_s e^{j\phi_s}, \quad (4)$$

where  $\alpha_s$  and  $\phi_s$  are the amplitude and phase of the static component.  $\alpha_d$  and  $\phi_d$  are the amplitude and phase of the dynamic component. As shown in Fig. 6(b), the curve shape of the dynamic component in the complex domain is determined by both amplitude and phase.

**Different Eye Rotation Directions.** For different directional movements of the eyeball, the folding of the eyelid and the rotation of the eyeball create a unique relative relationship, manifesting through the changes in IF signal amplitude and phase. We characterize this feature by utilizing the curvature of the curve. Specifically, we perform regression on the curve, identify an elliptical equation [8], and use the eccentricity of the ellipse to characterize this feature. As shown in Fig. 6(b), the ellipse generated by the up/down eye motions exhibits a more elongated shape, while the right/left motions lead to a more circular shape. This can be attributed to the fact that up/down eye motions involve more eyelid movements, leading to changes in reflective surface, while left/right eye rotations mainly cause changes in the length of the reflection path.

**Experimental Validation.** To verify the robustness of the amplitude and eccentricity features, we conduct experiments involving five participants. We repeat the experiments in the same setting as described above. Each participant performs his/her eye rotations in each direction 50 times. Then, we perform the kernel density estimation for all the participants. Fig. 6(c) presents the density estimation results of amplitude changing ratio. The up and down motions are centered on the 0.3 and -0.4, respectively. The left and right motions have a relatively smaller variation; and they are centered around zero. Fig. 6(d) shows the eccentricity density estimation results. The up/down motions are centered close to 1; and the left/right motions are close to 0.8. The statistical results across different individuals align with the findings described earlier for a single person. This consistency suggests the potential of segregating these motions based on the radar’s signal. To enhance the recognition of eye motions, we employ a DNN model, which will be described in §4.

### 3 RadEye: Signal Processing

In this section, we describe the signal processing of the radar’s IF signal for eye rotation detection. Fig. 7 shows the overall structure of the system. In what follows, we introduce the signal processing techniques for RadEye, which include the selection of the range bin and the extraction of eye motions.

**Range-FFT.** RadEye sets the chirp duration to 1 ms for detecting eye motions. In each cycle, the chirp takes 0.6 ms, and the delay takes 0.4 ms. RadEye employs a sample rate of 2.5 MSps to observe

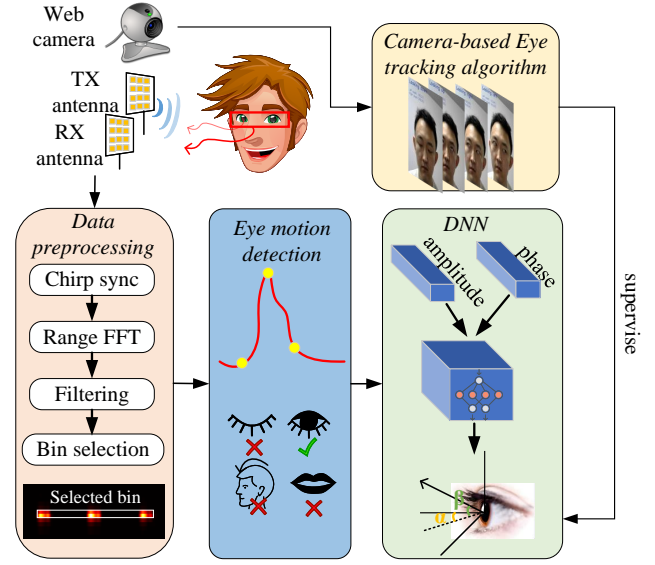


Figure 7: The system overview of RadEye.

the signal in the digital domain. Consequently, in each cycle, 1500 complex numbers are acquired. Subsequently, RadEye appends zeros to the end of the samples and performs a 4096-point range-FFT operation to obtain the signal at different ranges. In the 4096 bins, only the first 256 will be used since it already covers the range to 13 m.

**Filtering for Range-FFT.** RadEye applies a second-order Butterworth bandpass filter to suppress noise and out-of-band interference. It sets the filter’s pass band to 1 Hz~5 Hz [46, 50]. We note that, although the eye blink frequency may overlap with the chest breathing frequency (0.1 Hz~0.5 Hz), the input eye motion command for RadEye has a higher frequency and will not be affected by the filter. One may ask whether the heartbeat will cause the slight head shaking and thus pollute the eye motion signals, our answer is no. Based on our experimental results, the heartbeat is too weak to cause the head shaking that can be captured by RadEye.

**FFT Bin Selection.** Eye rotation motions have a very small dynamic range. Therefore, it is nontrivial to find the FFT bin that carries the eye motion features. To do so, RadEye requires users to blink their eyes three times with an interval of 2 seconds as a ‘start button’ to initiate the control process. The user only needs to provide the initialization command once. In this period, the users should keep their head still (no movement more than 14 cm). If the user’s head position moves beyond this range, the initialization command must be re-entered. Since this is a human input device, it is reasonable to require the user to remain relatively stationary within a short time period. RadEye utilizes the amplitude dynamic range as an indicator to find the candidate bin. The reason for using the amplitude is that, when the eyes switch between opening and closing, the blink motion causes the reflective surface to switch from the water-textured eyeball to the skin-textured eyelid [22], causing the amplitude change of the radar’s IF signal.

We describe the bin selection algorithm as follows. RadEye calculates the window-slides variance for each Range-FFT bin  $i$  by:

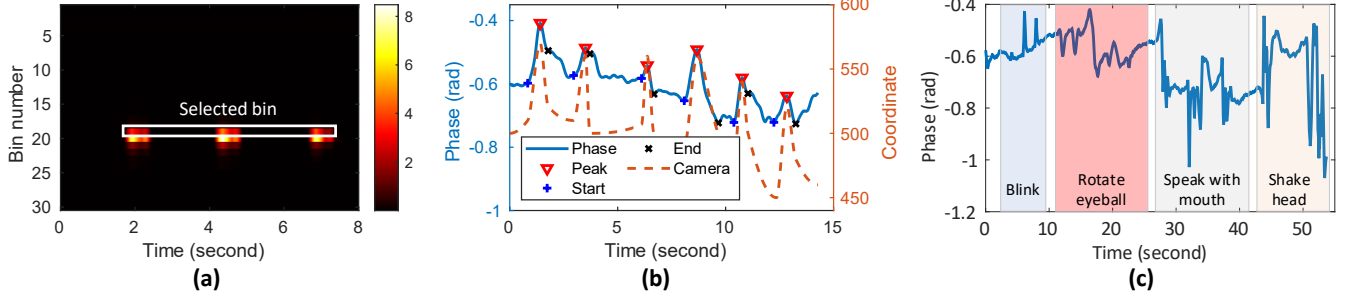


**Figure 8: (a) The signal amplitude variance for different Range-FFT bins during eye blinks. (b) Eye motion detected based on signal phase (with the camera-based ground truth marked). (c) Comparison of Eye motions and interfering motions from the target person's head.**

$v_i(j) = \frac{1}{W} \sum_{m=j}^{j+W-1} (|y_i(m)| - \bar{y}_i)^2$ , where  $\bar{y}_i = \frac{1}{W} \sum_{m=j}^{j+W-1} |y_i(m)|$ , and  $w$  is the window size which is set to 200 to fit the duration of the eye blink. If  $v_i(j)$  is larger than a predefined threshold  $T$ , the timestamp  $j$  will be recorded as  $t_n$ . Here,  $T$  is empirically set to 0.05. Only when the next detected timestamp  $j$  satisfies the  $2000 < j - t_n < 3000$  (fit in the interval of blink), it will be counted as the continuous blink. Once the three continuous blinks have been detected, we mark the Range-FFT bin  $i$  as the candidate bin. Multiple Range-FFT bins might satisfy this condition as shown in Fig. 8(a). In this case, RadEye chooses the bin that has the smallest index. The smallest-index Range-FFT bin represents the shortest path of signal travel, which best reflects the eye motion pattern.

**Eye Motion Detection.** After RadEye identifies the Range-FFT bin, it will continue to monitor this bin and estimate eye motions based on it. Each eye motion can be separated into three phases: start moving the eyeball, the eyeball reaches the edge, and the eyeball backs to the start position. RadEye tries to detect these three positions for each eye motion. Although both amplitude and phase contain information about eye motions, we found that phase exhibits a more significant pattern when detecting eye rotations.

Eyeball rotations involve repetitive movement. It rolls back to its central point when reaching the edge. This motion occurs swiftly, resulting in a repetitive phase change pattern. Hence, the positions of local phase extremums correspond to where eye movement reaches the edge. Additionally, we noticed that there are inflection points in the signal phase at the beginning and end of eye movements. RadEye utilizes these features to extract eye motions, it first searches for the local maximum/minimum on phase with an interval of 1 second. After identifying the local peaks, RadEye will search along the gradients of samples before/after the peak. The position in which the gradient is equal to zero will be defined as the start/end position. Fig. 8(b) presents the phase of the signal when a participant repeats the look-up motion, and the detected start, peak, and end positions are marked on the figure.

To mitigate interference from the target person's other body parts, we utilize both phase shift and time duration to refine the detection results. Fig. 8(c) shows eye blinks, eye rotations, head motions, and mouth motions. It can be seen that head and mouth motions induce significant changes in the signal phase. Consequently, if the phase shift surpasses a specified threshold, the signal is discarded. For motions falling below the threshold, the time duration is considered. Only signals within the duration range of

200 ms~600 ms are deemed as valid eye motion signals. Doing so will effectively filter out eye blinks, which typically last for less than 100 ms.

## 4 RadEye: DNN-based Eye Movement Detection

In this section, we present a DNN model for eye rotation recognition by using the amplitude and phase of the radar's IF signal. RadEye utilizes a transformer encoder to extract features and feeds these features into a fully connected layer to output the azimuth and elevation angles of a target person's eyeball. The DNN is trained using a camera-guided method, transferring the knowledge from computer vision to radio sensing.

### 4.1 Sequential Signal

The input signal to our DNN model is a time-series signal with a high sampling rate. As the subject's eyeballs rotate toward different angles, the swift motions of the eyeballs and eyelids cause fluctuations in the amplitude and phase of the input signal over time. Therefore, to accurately model the temporal dependencies between various sampling points, we employ a DNN model that is capable of efficiently encoding information over the temporal domain.

Traditional time-series models, such as Recurrent Neural Network (RNN) [26] and LSTM [12], are capable of temporal sequence modeling. However, they struggle with gradient vanishing and exploding problems when dealing with long sequence inputs, limiting their capabilities of capturing dependencies over a long distance. In contrast, Transformer [34], employing a self-attention mechanism, can effectively overcome these issues. The self-attention mechanism allocates a weight to the output of each position in a time series, reflecting the degree of attention that the position pays to other positions within the sequence. This method allows for the computation of correlations between any two positions in the sequence without being constrained by their physical separation, thus better capturing long-range dependencies. Furthermore, the multi-head attention mechanism within Transformers can project eye movement signals into various subspaces, including different frequency spaces. Frequency analysis can better distinguish certain angle information, as the movement of the eyeball at different angles will have different speeds.

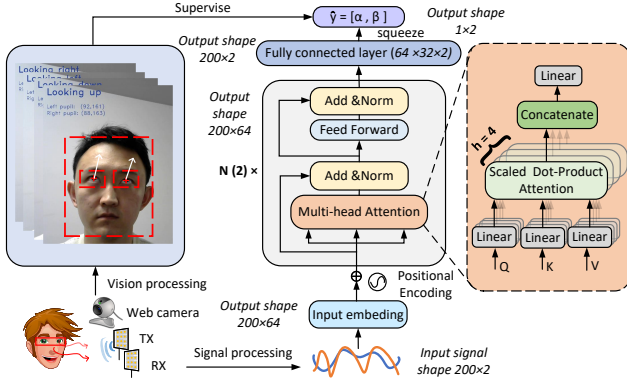


Figure 9: A camera-guided DNN structure for RadEye.

## 4.2 Camera-guided DNN Framework

The overall structure of our designed model, as shown in Fig. 9, primarily utilizes Transformer to predict an angle vector based on the input time-series data, which includes both the amplitude and phase derived from the corresponding Range-FFT bin. We introduce its key elements as follows.

- **Input Data.** The input data for the eye motion signal is captured by RadEye from the corresponding Range-FFT bin. Each input data sample consists of  $200 \times 2$  dimensions, where 200 is the time length of the data sample, and 2 is the number of features: amplitude and phase. The data have been normalized to ensure that they share the same dynamic range.
- **Signal Encoder.** Before sending to Transformer, the signal data are first passed through a projection layer to up-sample them to a higher-dimensional representation. The output size of this projection layer is  $200 \times 64$ . Additionally, to enable the model to discern the temporal relationships within the input sequence embeddings, each signal representation is augmented with positional embeddings.
- **Backbone.** The transformer encoder can extract features from the embedded data. RadEye uses two transformer encoders; and each encoder has four heads. The self-attention mechanism in the transformer encoder can build connections across different time steps in the signal and also attend to different parts of the signal. These connections enable the model to easily derive information about the eye rotation angle.
- **Prediction Head.** The extracted features finally feed into the fully connected layer, which has a size of  $64 \times 32 \times 2$ . It combines features from previous layers and flattens the output into the appropriate shape. The output of the model is a direction vector  $y = [\alpha, \beta]$ , where  $\alpha$  is the eyeball’s azimuth angle and the  $\beta$  is the eyeball’s elevation angle.
- **Camera-guided Training.** The vision processing module initially tracks the user’s face and subsequently localizes the position of the eyes. It then calculates the eye rotation angle based on the relative position of the pupil within the eye region. Guided by these vision-based techniques, the DNN model endeavors to create a feature extractor similar to those used in vision processing, but specifically designed to handle RF signals. The vision processing module ultimately provides the ground truth angle to the DNN, which then utilizes Mean Squared Error (MSE) to

calculate the loss for angle estimation. The loss function is as follows:

$$\mathcal{L}_{angle} = \frac{1}{N} \sum_{i=1}^N (y_i - \hat{y}_i)^2, \quad (5)$$

where  $y_i$  is the predicted angle vector and the  $\hat{y}_i$  is the ground truth angle vector.

## 4.3 Data Collection

We gathered training data exclusively in a controlled laboratory setting, where participants engaged with the radar and camera setup positioned on a table before them. Participants were seated 3 m away from the radar, facing it directly as shown in Fig. 10(a). A total of 8 participants took part in the data collection. In each data collection session, participants were instructed to rotate their eyes in up, down, right, and left directions. Recognizing the potential fatigue associated with eye rotation, each test session had a limited duration of 3 minutes. Each participant will repeat 15 sessions, generating a total of 27,000 data samples.

We note that during the test phase, the eye motion signals are directly captured using RadEye (no camera presents). In this scenario, the length of the signal vector may differ from the training data. To ensure consistent input dimensions, downsampling or interpolation techniques are employed to normalize the data dimension.

## 5 Experimental Evaluation

In this section, we conduct experiments to evaluate the performance of RadEye. Particularly, we aim to answer the following questions.

- **Q1 (§5.4):** What is RadEye’s detection rate of eye motions?
- **Q2 (§5.5):** What is RadEye’s accuracy in estimating eye rotation angles?
- **Q3 (§5.6):** What is RadEye’s resilience to environmental changes and interference?
- **Q4 (§5.7):** What is RadEye’s zero-shot performance (for unseen users and in unseen scenarios)?

### 5.1 Implementation

**Hardware.** Fig. 11 shows the hardware of RadEye. We have a fabricated a PCB board capable of transmitting and receiving FMCW signals at 5 GHz, using Wi-Fi’s electronic components. The received signal undergoes amplification with a power amplifier (PA), and then it is mixed with the transmitted signal. The electronic components of this board also include Tx/Rx 16 dB coupling, RF I/Q mixer, and baseband filtering. Additionally, we have custom-designed and optimized a  $4 \times 4$  patch antenna using HFSS for signal transmission and reception. A single patch antenna provides an 15 dBi gain, resulting in a total gain of 30 dBi. The patch antenna design maintains the signal beam within a narrow range while providing significant gain, enabling RadEye to detect eye motions from a distance. The mixed signal is subsequently fed into a USRP N210 with an LFRX daughterboard to convert the analog signal into baseband I/Q samples. The FMCW signal generated by RadEye sweeps from 5.4 GHz to 6.5 GHz. Each chirp has a time duration of 1 ms, with 600  $\mu$ s for frequency ramping and 400  $\mu$ s idle.

**Software.** We implemented our data preprocessing module in C++ using the GNURadio out-of-tree module. A crucial function



Figure 10: Experiment settings in a lab for different distances and angles. (a) 3 meters. (b) 4 meters (c) 5 meters. (d) 15°. (e) 30°.

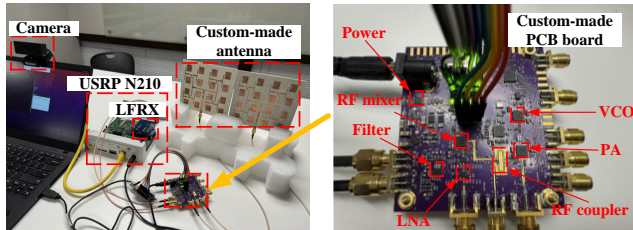


Figure 11: The system setting for RadEye.

of this module is to synchronize the chirps, facilitating the extraction of useful samples. However, owing to the absence of clock synchronization between the USRP ADC and FMCW chirps, only the software-based method can be employed for synchronization. To address this issue, we utilize a high-sampling rate of 2.5 MSPs and the idle period for synchronization. Initially, we detect the idle period based on the smooth amplitude during this interval, followed by fine-grained detection to identify the first sample of the chirp. The DNN model was implemented using PyTorch with the Adam optimizer. Throughout the training process, a batch size of 200 and 50 epochs were set.

## 5.2 Experimental Setting

During the experiments, participants were seated on a chair facing the antennas of RadEye. The antennas were positioned 1.1 m above the ground on a tripod. A varifocal camera was placed on top of the laptop to capture the participants' face video for their eye motion detection using the SOTA gaze tracking tool [17]. Our experimental studies show that this camera-based eye detection tool achieves about 98% accuracy as shown in Fig. 13. While it is not perfect, we use the detection results from the camera-based tool as the ground-truth labels to supervise the training of RadEye's DNN model. During the inference, we also use the camera-based detection results as the ground-truth to evaluate the estimation accuracy of RadEye.

RadEye and camera operated concurrently, synchronized with the PC clock, to estimate participants' eye rotations. RadEye, with a higher sample rate than the camera's frame rate (10 frames/s), resulted in each camera-captured direction being mapped to 200 continuous chirps. Each training sample in our dataset is a  $200 \times 2$  matrix, where 200 is the time dimension, and 2 is the feature dimensions (azimuth and elevation).

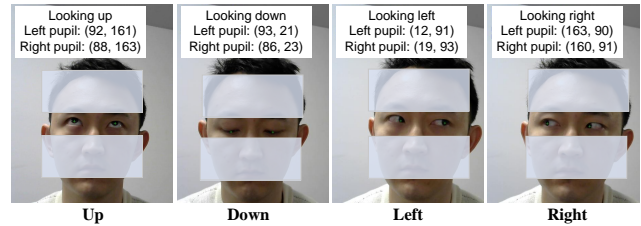


Figure 12: The eye rotation directions captured by a camera. It is used as ground truth for DNN training and evaluation.

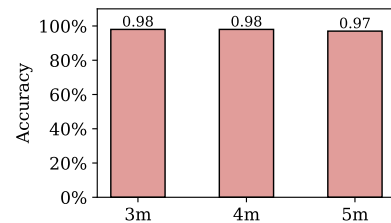
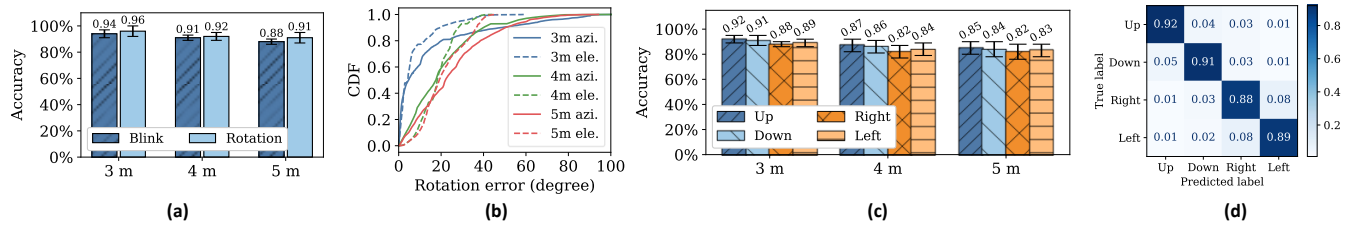


Figure 13: Tracking accuracy of eye rotation with camera at varying distances.

## 5.3 Performance Metrics

We consider the following three performance metrics.

- **Eye Motion Detection Rate (EMR).** The eye motion here is defined as the eye blink and eye rotation. The signal processing module extracts the eye motion signals from RF data before sending them to the DNN model. We define  $Detection\ rate = \frac{Number\ of\ eye\ motions\ detected}{Total\ eye\ motions\ performed}$ .
- **Estimation Error of Eye Rotation Angle (ERA).** The eye rotation angles are illustrated in the bottom right corner of Fig. 7. The estimation error of azimuth angle is defined as  $e_\alpha = |\alpha - \hat{\alpha}|$ , where  $\hat{\alpha}$  is the estimated eye rotation azimuth angle and  $\alpha$  is the eye rotation angle ground truth provided by the camera. Similarly, the estimation error of elevation angle is defined as:  $e_\beta = |\beta - \hat{\beta}|$ .
- **Estimation Accuracy of Eye Rotation Direction (ERD).** Some applications of RadEye (e.g., remote TV control) may not require precise angle measurements for functionality but instead focus on eye rotation direction. This metric evaluates the accuracy of classifying eye movement directions into four categories: up, down, left, and right. Specifically, we define  $Accuracy = \frac{Number\ of\ correct\ direction\ estimations}{Total\ eye\ rotations\ performed}$ .



**Figure 14: (a) RadEye’s eye blink/rotation detection rate. (b) RadEye’s eye rotation estimation error at different distances. (c) RadEye’s accuracy of estimating eye rotation directions. (d) The confusion matrix of RadEye’s eye rotation direction estimation at 3 m distance.**

## 5.4 Eye Motion Detection Rate

RadEye’s eye motion detection ability, including eye rotation and eye blink detection, serves as the foundation of many eye tracking applications. While RadEye focuses on estimating eye rotation angles, eye blink detection is also one of its key components. This feature not only enhances the input of RadEye but also enriches its functionalities. Therefore, we evaluate RadEye’s success rate of detecting eye rotation and blink.

We instructed eight participants to perform eye rotations and blinks from three different distances: 3 m, 4 m, and 5 m, as shown in Fig. 10(a)-(c). A total of 5 minutes of data were collected at each distance for each participant. Fig. 14(a) shows RadEye’s average eye motion detection rate for 8 individuals at various distances. The highest detection rate for eye blink and eye rotation is 94% and 96%, respectively. This was observed at the distance of 3 m. Overall, the detection rate is consistent. Even at a distance of 5 m, RadEye achieves 88% detection rate for eye blinks and 91% detection rate for eye rotation. This confirms the robustness of RadEye in eye motion detection in different environmental settings. Numerically, the standard deviation of eye blink detection across the eight individuals is about 2%. For the eye rotation detection, the standard deviation is about 4%. This slight difference can be attributed to the simplicity and similarity of eye blink motion across different individuals. Additionally, the detection rate of eye rotations is consistently higher than that of eye blinks in all cases. This is not surprising, as eye rotations involve more significant facial muscle movements compared to eye blinks.

## 5.5 Eye Rotation Angle/Direction Estimation

**Eye Rotation Angle Estimation.** We conducted the experiments in the same way as described in §5.4. Fig. 14(b) presents the cumulative distribution function (CDF) of the angle estimation errors of RadEye for all participants at three different distances. The mean azimuth/elevation errors at 3 m, 4 m, and 5 m are approximately  $14^\circ/7^\circ$ ,  $20^\circ/18^\circ$ , and  $24^\circ/21^\circ$ , respectively. Evidently, the eye rotation angle estimation error increases as the distance increases. This is not surprising, as the radio signal has a larger attenuation over a longer distance. Additionally, we observed that the elevation angle estimation error is consistently smaller than the azimuth angle estimation error. This observation agrees with our previous observation in §2, i.e., eye’s vertical movements (up and down) generate more pronounced changes in radar signal’s amplitude and phase compared to eye’s horizontal movements (right and left).

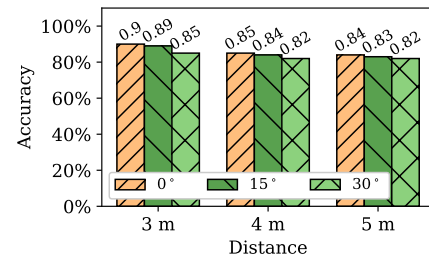


**Figure 15: RadEye’s estimation accuracy of eye rotation directions when the target person is located at different distances and angles.**

**Eye Rotation Direction Estimation.** As some applications of RadEye need only the eye rotation direction information, we first classify the estimated eye rotation angle into four directions (up, down, left, and right) and then evaluate the estimation accuracy. Since the slight eye motions are always accompanied by humans, we consider the eye rotation action effective only when the azimuth  $\alpha < 50^\circ$  or  $\alpha > 130^\circ$ , or the elevation  $\beta < 50^\circ$  or  $\beta > 130^\circ$ , as exemplified by Fig. 12. Using the effective input captured by the camera as ground truth, we can measure RadEye’s estimation accuracy. Fig. 14(c) plots the average estimation accuracy for eight people at three different distances. The average estimation accuracy at 3 m, 4 m, and 5 m is 90.0%, 84.7%, and 83.5%, respectively. These accuracy levels are suited for most daily applications requiring human input. The standard deviations at 3 m, 4 m and 5 m are 3%, 5% and 5.5%. This indicates RadEye’s robustness when detecting eye rotation of different users. Additionally, Fig. 14(d) presents the confusion matrix in the 3-meter case. It is evident that distinguishing between right and left eye rotations is more challenging compared to up and down eye rotations. This suggests that developing an application with binary input for up and down movements could enhance RadEye’s robustness.

## 5.6 RadEye’s Robustness

**RadEye’s Field of View.** RadEye has two patch antennas for signal transmission and reception. Ideally, the target person should be perpendicularly facing RadEye’s antenna. In practice, the target person may not be ideally positioned. Therefore, we conducted experiments to evaluate RadEye’s field of view by examining its estimation accuracy when the target person was located in different directions, as illustrated in Fig. 10(d)-(e). Specifically, five participants performed eye rotations at angles of  $15^\circ$  and  $30^\circ$  from three

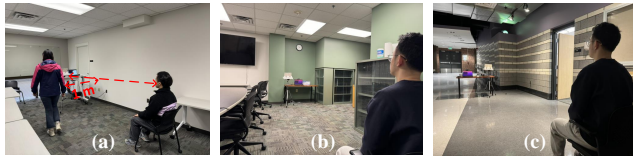


**Figure 16: (a) The interference test in a lab. (b) Test at 5 m in the conference room. (c) Test at 5 m in the hallway.**

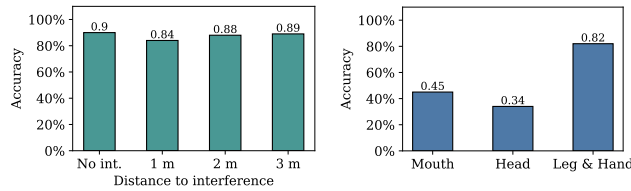


**Figure 17: RadEye's estimation accuracy of eye rotation directions when experiencing interference from walking people. Figure 18: RadEye's estimation accuracy of eye rotation directions during self-body motions.**

different distances. In total, six scenarios were studied. In each scenario, participants performed eye rotations for 5 minutes. Fig. 15 shows our experimental results. It can be seen that RadEye achieves a high estimation accuracy when the target person is located at  $0^\circ$ ,  $15^\circ$ , and  $30^\circ$ . Overall, the estimation accuracy remains above 82% in all cases. This indicates that RadEye has at least  $60^\circ$  field of view.

**Impact of Moving Objects.** Since static objects can easily be filtered out in the received signal, we further evaluated RadEye's resilience to interference caused by nearby walking individuals. In the experiments, another person was asked to walk around the user in close proximity, as depicted in Fig. 16(a). We measured the accuracy in three scenarios where the distance between the user and the walking person was 1 m, 2 m, and 3 m. In each scenario, five participants performed eye rotations for 5 minutes. Fig. 17 shows the results. The presence of a walking person causes a slight decrease in RadEye's estimation accuracy. Overall, RadEye achieves accuracies of 84%, 88%, and 89% when the walking person is 1 m, 2 m, and 3 m away from the participant, respectively. We note that all these experiments were conducted in normal scenarios. The participants were only instructed to keep their heads still when performing eye rotations. No other restrictions were made to avoid interference from multipath effects or other normal physiological activities of the participants.

**Impact of Self-Body Motions.** Besides nearby moving objects, the participant's own body movements may also affect RadEye's performance. To evaluate RadEye's usability in practical scenarios, we studied the cases where the participant was speaking, shaking head, or engaging in leg or hand motions. A participant was asked to perform these three activities separately while executing eye rotations. In each scenario, the participant performed eye rotations for five minutes at a distance of 3 m. Fig. 18 presents our measurement results. It can be seen that RadEye's accuracy remains at 82% when the participant performed leg or hand motions. However, RadEye's accuracy decreases to 34% when he was shaking his head and to 45% when he was speaking. This reduction could be attributed to

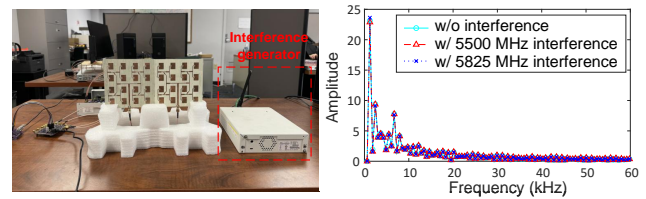


**Figure 19: Wi-Fi interference test: experimental setup (left) and experimental results (right).**

the limited resolution of RadEye. Since the legs and hands are more than 14 cm away from the eyes, their movements have minimal impact on RadEye's detection accuracy. However, head and mouth movements interfere with the eye rotation signal, leading to a lower detection accuracy.

**Impact of Wi-Fi signals.** As RadEye operates at 5 GHz, overlapping with part of the Wi-Fi spectrum, we conducted experiments to evaluate the impact of Wi-Fi signal interference on RadEye. A Wi-Fi interferer was set up using the USRP and placed next to RadEye, as shown in Fig. 19, continuously transmitting Wi-Fi packets. The Wi-Fi signals were generated at two frequencies, 5.5 GHz and 5.825 GHz, with a bandwidth of 20 MHz. The experiments were conducted in a static environment. We compared the IF signals from RadEye with and without Wi-Fi interference, and the results are shown in Fig. 19. We observed that the IF signals remain nearly identical, regardless of the presence of Wi-Fi signals.

RadEye appears to be resilient to Wi-Fi interference due to two key factors. First, RadEye operates with a broad bandwidth of 1.1 GHz, whereas Wi-Fi signals occupy only 20 MHz. Second, RadEye employs FMCW modulation, which contrasts with Wi-Fi's OFDM modulation. OFDM signals exhibit pseudo-noise characteristics, and when they are correlated with FMCW signals over time, the resulting correlation is close to zero. This theoretical outcome explains why RadEye can effectively resist interference from nearby Wi-Fi devices.

## 5.7 Zero-Shot Performance

Since RadEye has a DNN component for eye rotation detection, it is critical to evaluate its zero-shot performance against new users and new scenarios.

**New Users.** The generality of the trained model is crucial as it allows for easy extension to new users with minimal effort. To evaluate this, we conducted a cross-user test for RadEye. Specifically, four new users who were not involved in the training data collection were invited to perform eye rotations at a distance of 5 m. Among these users, participants B and C wore glasses. Each participant contributed 5 minutes of data. Fig. 20 reports RadEye's estimation accuracy for these four different users. The highest accuracy is 86% for user A, and the lowest accuracy is 77% for user D. Notably, wearing glasses does not seem to affect the results much. RadEye achieves an average accuracy higher than 80% for new users. This demonstrates the generalizability of RadEye to new users.

**New Environments.** In addition to evaluating RadEye's generalizability to new users, we also assessed its zero-shot performance in unseen scenarios. Four new participants performed eye

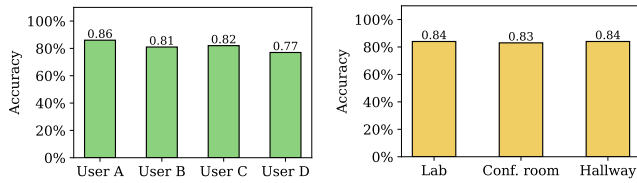


**Figure 20: The accuracy for users not in the training set.**

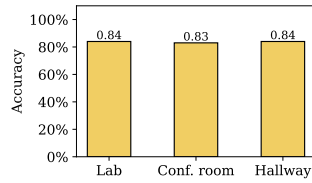


**Figure 21: The accuracy in the different environments.**

rotations at a distance of 5 m in both a conference room and a hallway. Fig. 16(b)-(c) illustrates our experimental settings, where participants faced RadEye at an angle of  $0^\circ$ . Fig. 21 presents the measurement results. RadEye achieves accuracies of 83% and 84% in the conference room and hallway, respectively. These results demonstrate RadEye’s ability to generalize to unseen environments as well.

## 6 Related Work

### 6.1 Eye Motion Recognition

**Acoustic-based Detection.** As speakers and microphones are now commonplace on mobile devices, acoustic signals have become widely utilized for recognizing human daily activities. BlinkListener [22] can detect eye blink motions using acoustic signals, modeling variations caused by eye blinks and interference. By leveraging interference, they identify an optimal position to maximize the variation induced by eye blinks. TwinkleTwinkle [5] addresses a similar objective using a different approach. They employ a phase difference-based method to detect potential blink motions, followed by a model-based approach to distinguish subtle motions. Additionally, they establish a language input system based on ASCII code and Morse code. While RadEye is capable of recognizing eye motions, the mentioned works focus solely on detecting eye blinks at limited distances.

**RF-based Detection.** In the study by Zhang et al. [47], an off-the-shelf mmWave FMCW radar is employed to detect eye blinks. They introduce an Adaptive Variational Mode Decomposition (AVMD) algorithm to extract the blink signal, achieving an effective detection distance of up to 1.2 meters. Several other studies [3, 24, 39] have taken a similar approach with mmWave FMCW radar. In addition to the mmWave signal, BlinkRadar [13] employs UWB radar to detect eye blinks in a driving scenario. They implemented a customized impulse-radio ultra-wideband (IR-UWB) radar. By analyzing signal features in the complex domain, the system can isolate eye blinks without interference from other motions.

**Camera-based Detection.** Due to the ubiquity of web cameras and smartphone cameras, significant progress has been made in using cameras to track eye motion. In the computer vision research domain, deep learning networks have been effectively employed to predict gaze direction [16, 30, 49, 51]. Furthermore, in the security domain, studies have shown that the camera on a mobile phone can even track the gaze trace, raising concerns about potential password leakage [4, 38]. Additionally, there are commercial eye-trackers available on the market [10, 33] that support high-accuracy eye-tracking at an affordable price. However, it’s worth noting that all camera-based eye-tracking solutions may raise privacy concerns and may not function effectively in low-light scenarios.

**Wearable-based Detection.** With the prevalence of VR devices, smart glasses offer another solution for eye motion detection. Google Glass [14] and Jins MEME pair of eyeglasses [6] demonstrated the potential to detect eye motions several years ago. Building on existing approaches, Liu et al. [23] attached a copper electrode to the glass frame to sense eye blinks by utilizing the capacitance variation between the electrode and eyelid. However, wearable devices like these require users to keep the glasses on their heads, which may be inconvenient for daily use.

### 6.2 Fine-grained HAR

**MmWave-based Recognition.** MmWave FMCW radar has reached great performance these years due to its fine-grained detection ability and affordable cost. They are extensively used in human activity recognition and vital sign detection [11, 21, 41, 42, 48, 50]. Thanks to their substantial bandwidth and diminutive wavelength, they attain millimeter-level accuracy in detecting object movements.

**Wi-Fi-based Recognition.** Channel State Information (CSI) in Wi-Fi networks has been applied across various sensing applications, including gesture recognition [9, 19, 45], vital sign detection [37], and radio imaging [15, 20, 29, 36]. Nevertheless, Wi-Fi, characterized as a non-coherent system due to the physical separation of its transmitter and receiver, faces limitations in detection accuracy stemming from timing, frequency, and phase misalignments.

## 7 Limitations and Discussions

In this section, we point out the limitations of RadEye and discuss potential solutions to address them.

- **Interference caused by head and mouth movements.** While RadEye is resilient to interference from surrounding environments, it requires the users to keep their heads still during use. Movements such as head shaking, speaking, or other facial expressions can obscure the eye rotation signals, resulting in unsuccessful detection. To address this issue, one approach is to increase the bandwidth of RadEye. When the bandwidth is sufficiently large, RadEye can differentiate eyes from mouth in the frequency domain, thereby eliminating the interference from head and mouth movements for eye motion detection.
- **RadEye versus mmWave radar.** MmWave radar is capable of detecting subtle movements, such as eye motion, and is commercially available on the market. However, its detection range is relatively short due to the rapid signal attenuation of mmWave propagation. In contrast, RadEye offers a significantly larger range for eye motion detection but requires a wide spectrum bandwidth at lower frequencies. Therefore, both mmWave radar and RadEye have distinct advantages and limitations. MmWave radar is better suited for short-range eye tracking, while RadEye is more appropriate for long-range use cases.
- **Physical size of RadEye.** Our current prototype of RadEye is not compact enough for certain applications, such as installation on wheelchairs. This limitation arises because our prototype has not yet been optimized. In fact, the current design has significant potential for size reduction through various optimizations, including using smaller packages (e.g., SMD) for electronic components, more efficient power management chips, improved

patch antenna designs, and shorter cables. Moreover, integrating the patch antennas directly into the PCB could significantly reduce the system's physical size, making it more suitable for space-constrained applications.

- **User fatigue.** RadEye currently recognizes eye rotations in only four directions, requiring users to rotate their eyes multiple times to input a word. This tends to cause eye fatigue. Future work will focus on developing a system capable of continuously tracking eye rotation directions with high accuracy, rather than limiting recognition to four discrete directions. This improvement would enhance input efficiency and significantly reduce user fatigue.

## 8 Conclusion

Remote eye tracking has many potential applications ranging from HCI-based input to eye disease detection. While camera has been widely studied for eye tracking, its application in practice may raise privacy concerns in some scenarios. In this paper, we presented RadEye, an RF sensing system capable of recognizing fine-grained human eye movement from a long distance. The challenge in the design of RadEye is to detect tiny eyeball movements in the presence of interference from other moving objects. RadEye addresses this challenge through a joint hardware and software design. For hardware, RadEye custom-designed a sub-6GHz FMCW radar for feature extraction and interference mitigation. For software, a camera-guided DNN model has been crafted to improve RadEye's detection accuracy. Extensive experiments show that RadEye achieves 90% accuracy when detecting people's eye rotation directions (up, down, left, and right) in various scenarios.

## Acknowledgments

We sincerely thank the anonymous reviewers for their insightful comments. This project was supported in part by NSF Grant ECCS-2225337.

## References

- [1] ALS news today. 2024. ALS Facts and Statistics. <https://tinyurl.com/bs8rmh3w>. [Online; accessed 11-September-2024].
- [2] Amy Yee. 2024. Why Do Eye Muscles Function in ALS as Other Muscles Waste Away? <https://tinyurl.com/37tk2rm4>. [Online; accessed 11-September-2024].
- [3] Emanuele Cardillo, Gaia Sapienza, Changzhi Li, and Alina Caddemi. 2021. Head motion and eyes blinking detection: A mm-wave radar for assisting people with neurodegenerative disorders. In *2020 50th European Microwave Conference (EuMC)*. IEEE, Piscataway, NJ, USA, 925–928. doi:10.23919/EuMC48046.2021.9338116
- [4] Yimin Chen, Tao Li, Rui Zhang, Yanchao Zhang, and Terri Hedgpath. 2018. Eyetell: Video-assisted touchscreen keystroke inference from eye movements. In *2018 IEEE Symposium on Security and Privacy (SP)*. IEEE, Piscataway, NJ, USA, 144–160. doi:10.1109/SP.2018.00010
- [5] Haiming Cheng, Wei Lou, Yanni Yang, Yi-pu Chen, and Xinyu Zhang. 2023. TwinkleTwinkle: Interacting with Your Smart Devices by Eye Blink. *Proceedings of the ACM on Interactive, Mobile, Wearable and Ubiquitous Technologies* 7, 2 (2023), 1–30. doi:10.1145/3596238
- [6] Murtaza Dhuliawala, Juyoung Lee, Junichi Shimizu, Andreas Bulling, Kai Kunze, Thad Starner, and Woontack Woo. 2016. Smooth eye movement interaction using EOG glasses. In *Proceedings of the 18th ACM International Conference on Multimodal Interaction*. Association for Computing Machinery, New York, NY, USA, 307–311. doi:10.1145/2993148.2993181
- [7] Yuda Feng, Yaxiong Xie, Deepak Ganesan, and Jie Xiong. 2021. LTE-based pervasive sensing across indoor and outdoor. In *Proceedings of the 19th ACM Conference on Embedded Networked Sensor Systems*. Association for Computing Machinery, New York, NY, USA, 138–151. doi:10.1145/3485730.3485943
- [8] Andrew Fitzgibbon, Maurizio Pilu, and Robert B Fisher. 1999. Direct least square fitting of ellipses. *IEEE Transactions on pattern analysis and machine intelligence* 21, 5 (1999), 476–480. doi:10.1109/34.765658
- [9] Zhangjie Fu, Jiashuang Xu, Zhuangdi Zhu, Alex X Liu, and Xingming Sun. 2018. Writing in the air with WiFi signals for virtual reality devices. *IEEE Transactions on Mobile Computing* 18, 2 (2018), 473–484. doi:10.1109/TMC.2018.2831709
- [10] GazeRecorder. 2024. Online Eye Tracking Software. <https://gazerecorder.com/>. [Online; accessed 6-September-2024].
- [11] Unsoo Ha, Salah Assana, and Fadel Adib. 2020. Contactless seismocardiography via deep learning radars. In *Proceedings of the 26th annual international conference on mobile computing and networking*. Association for Computing Machinery, New York, NY, USA, 1–14. doi:10.1145/3372224.3419982
- [12] Sepp Hochreiter and Jürgen Schmidhuber. 1997. Long short-term memory. *Neural computation* 9, 8 (1997), 1735–1780.
- [13] Jingyang Hu, Hongbo Jiang, Daibo Liu, Zhu Xiao, Schahram Dustdar, Jiangchuan Liu, and Geyong Min. 2022. BlinkRadar: non-intrusive driver eye-blink detection with UWB radar. In *2022 IEEE 42nd International Conference on Distributed Computing Systems (ICDCS)*. IEEE, Piscataway, NJ, USA, 1040–1050. doi:10.1109/ICDCS54860.2022.00104
- [14] Shoya Ishimaru, Kai Kunze, Koichi Kise, Jens Weppner, Andreas Dengel, Paul Lukowicz, and Andreas Bulling. 2014. In the blink of an eye: combining head motion and eye blink frequency for activity recognition with google glass. In *Proceedings of the 5th augmented human international conference*. Association for Computing Machinery, New York, NY, USA, 1–4. doi:10.1145/2582051.2582066
- [15] Wenjun Jiang, Hongfei Xue, Chenglin Miao, Shiyang Wang, Sen Lin, Chong Tian, Srinivasan Murali, Haochen Hu, Zhi Sun, and Lu Su. 2020. Towards 3D human pose construction using WiFi. In *Proceedings of the 26th Annual International Conference on Mobile Computing and Networking*. Association for Computing Machinery, New York, NY, USA, 1–14. doi:10.1145/3372224.3380900
- [16] Kyle Krafka, Aditya Khosla, Petr Kellnhofer, Harini Kannan, Suchendra Bhandarkar, Wojciech Matusik, and Antonio Torralba. 2016. Eye tracking for everyone. In *Proceedings of the IEEE conference on computer vision and pattern recognition*. IEEE, Piscataway, NJ, USA, 2176–2184. doi:10.1109/CVPR.2016.239
- [17] Antoinelame Antoine Lamé. 2024. Gaze Tracking. <https://github.com/antoinelame/GazeTracking>. [Online; accessed 11-September-2024].
- [18] Kyoung-Min Lee, Annie P Lai, James Brodale, and Arthur Jampolsky. 2007. Sideslip of the medial rectus muscle during vertical eye rotation. *Investigative ophthalmology & visual science* 48, 10 (2007), 4527–4533.
- [19] Chenning Li, Manni Liu, and Zhichao Cao. 2020. WiHF: Enable user identified gesture recognition with WiFi. In *IEEE INFOCOM 2020-IEEE Conference on Computer Communications*. IEEE, Piscataway, NJ, USA, 586–595. doi:10.1109/INFOCOM41043.2020.9155539
- [20] Chenning Li, Zheng Liu, Yuguang Yao, Zhichao Cao, Mi Zhang, and Yunhao Liu. 2020. Wi-fi see it all: generative adversarial network-augmented versatile wi-fi imaging. In *Proceedings of the 18th Conference on Embedded Networked Sensor Systems*. Association for Computing Machinery, New York, NY, USA, 436–448. doi:10.1145/3384419.3430725
- [21] Zhengxiong Li, Fenglong Ma, Aditya Singh Rathore, Zhuolin Yang, Baicheng Chen, Lu Su, and Wenyao Xu. 2020. Wavespy: Remote and through-wall screen attack via mmwave sensing. In *2020 IEEE Symposium on Security and Privacy (SP)*. IEEE, Piscataway, NJ, USA, 217–232. doi:10.1109/SP40000.2020.00004
- [22] Jialin Liu, Dong Li, Lei Wang, and Jie Xiong. 2021. BlinkListener: "Listen" to Your Eye Blink Using Your Smartphone. *Proceedings of the ACM on Interactive, Mobile, Wearable and Ubiquitous Technologies* 5, 2 (2021), 1–27. doi:10.1145/3463521
- [23] Mengxi Liu, Sizhen Bian, and Paul Lukowicz. 2022. Non-contact, real-time eye blink detection with capacitive sensing. In *Proceedings of the 2022 ACM International Symposium on Wearable Computers*. Association for Computing Machinery, New York, NY, USA, 49–53. doi:10.1145/3544794.3558462
- [24] Lina Ma, Yangtao Ye, Changzhan Gu, and Junfa Mao. 2022. High-Accuracy Contactless Detection of Eyes' Activities based on Short-Range Radar Sensing. In *2022 IEEE MTT-S International Microwave Biomedical Conference (IMBioC)*. IEEE, Piscataway, NJ, USA, 266–268. doi:10.1109/IMBioC52515.2022.9790181
- [25] Rima-Maria Rahal and Susann Fiedler. 2019. Understanding cognitive and affective mechanisms in social psychology through eye-tracking. *Journal of Experimental Social Psychology* 85 (2019), 103842.
- [26] David E Rumelhart, Geoffrey E Hinton, Ronald J Williams, et al. 1985. Learning internal representations by error propagation.
- [27] Cian Ryan, Brian O'Sullivan, Amr Elrasad, Aisling Cahill, Joe Lemley, Paul Kieley, Christoph Posch, and Etienne Perot. 2021. Real-time face & eye tracking and blink detection using event cameras. *Neural Networks* 141 (2021), 87–97.
- [28] Science Daily. 2024. Eye muscles are resilient to ALS. <https://tinyurl.com/cy4kxhv2>. [Online; accessed 11-September-2024].
- [29] Kunzhe Song, Qijun Wang, Shichen Zhang, and Huacheng Zeng. 2024. SiWiS: Fine-grained Human Detection Using Single WiFi Device. In *Proceedings of the 30th Annual International Conference on Mobile Computing and Networking*. Association for Computing Machinery, New York, NY, USA, 1439–1454. doi:10.1145/3636534.3690703
- [30] Yusuke Sugano, Yasuyuki Matsushita, and Yoichi Sato. 2014. Learning-by-synthesis for appearance-based 3d gaze estimation. In *Proceedings of the IEEE conference on computer vision and pattern recognition*. IEEE, Piscataway, NJ, USA, 1821–1828. doi:10.1109/CVPR.2014.235
- [31] Koh Tadokoro, Toru Yamashita, Yusuke Fukui, Emi Nomura, Yasuyuki Ohta, Setsuko Ueno, Saya Nishina, Keiichiro Tsunoda, Yosuke Wakutani, Yoshiki Takao,

- et al. 2021. Early detection of cognitive decline in mild cognitive impairment and Alzheimer's disease with a novel eye tracking test. *Journal of the neurological sciences* 427 (2021), 117529.
- [32] Texas Instruments. 2024. TI AWR6843. <https://www.ti.com/tool/AWR6843ISK>. [Online; accessed 11-September-2024].
- [33] Tobii. 2024. TOBII PRO SPECTRUM. <https://www.tobii.com>. [Online; accessed 11-September-2024].
- [34] Ashish Vaswani, Noam Shazeer, Niki Parmar, Jakob Uszkoreit, Llion Jones, Aidan N. Gomez, Łukasz Kaiser, and Illia Polosukhin. 2017. Attention is all you need. In *NIPS'17* (Long Beach, California, USA). Curran Associates Inc., Red Hook, NY, USA, 6000–6010.
- [35] Chuyu Wang, Lei Xie, Yuancan Lin, Wei Wang, Yingying Chen, Yanling Bu, Kai Zhang, and Sanglu Lu. 2021. Thru-the-wall eavesdropping on loudspeakers via RFID by capturing sub-mm level vibration. *Proceedings of the ACM on Interactive, Mobile, Wearable and Ubiquitous Technologies* 5, 4 (2021), 1–25. doi:10.1145/3494975
- [36] Fei Wang, Sanping Zhou, Stanislav Panev, Jinsong Han, and Dong Huang. 2019. Person-in-WiFi: Fine-grained person perception using WiFi. In *Proceedings of the IEEE/CVF International Conference on Computer Vision*. IEEE, Piscataway, NJ, USA, 5452–5461. doi:10.1109/ICCV.2019.00555
- [37] Xuyu Wang, Chao Yang, and Shiwen Mao. 2017. PhaseBeat: Exploiting CSI phase data for vital sign monitoring with commodity WiFi devices. In *2017 IEEE 37th International Conference on Distributed Computing Systems (ICDCS)*. IEEE, Piscataway, NJ, USA, 1230–1239. doi:10.1109/ICDCS.2017.206
- [38] Yao Wang, Wandong Cai, Tao Gu, and Wei Shao. 2019. Your eyes reveal your secrets: An eye movement based password inference on smartphone. *IEEE transactions on mobile computing* 19, 11 (2019), 2714–2730.
- [39] Yong Wang, Yuhong Shu, and Mu Zhou. 2021. A Novel Eye Blink Detection Method using Frequency Modulated Continuous Wave Radar. In *2021 IEEE International Workshop on Electromagnetics: Applications and Student Innovation Competition (IWEM)*. IEEE, Piscataway, NJ, USA, 1–3. doi:10.1109/IWEM53379.2021.9790529
- [40] Zhiqing Wei, Yuan Wang, Liang Ma, Shaoshi Yang, Zhiyong Feng, Chengkang Pan, Qixun Zhang, Yajuan Wang, Huici Wu, and Ping Zhang. 2022. 5G PRS-based sensing: A sensing reference signal approach for joint sensing and communication system. *IEEE Transactions on Vehicular Technology* 72, 3 (2022), 3250–3263.
- [41] Jiahong Xie, Hao Kong, Jiadi Yu, Yingying Chen, Linghe Kong, Yanmin Zhu, and Feilong Tang. 2023. mm3DFace: Nonintrusive 3D Facial Reconstruction Leveraging mmWave Signals. In *Proceedings of the 21st Annual International Conference on Mobile Systems, Applications and Services*. Association for Computing Machinery, New York, NY, USA, 462–474. doi:10.1145/3581791.3596839
- [42] Hongfei Xue, Yan Ju, Chenglin Miao, Yijiang Wang, Shiyang Wang, Aidong Zhang, and Lu Su. 2021. mmMesh: Towards 3D real-time dynamic human mesh construction using millimeter-wave. In *Proceedings of the 19th Annual International Conference on Mobile Systems, Applications, and Services*. Association for Computing Machinery, New York, NY, USA, 269–282. doi:10.1145/3458864.3467679
- [43] Lei Yang, Qiongzhen Lin, Xiangyang Li, Tianci Liu, and Yunhao Liu. 2015. See through walls with COTS RFID system!. In *Proceedings of the 21st Annual International Conference on Mobile Computing and Networking*. Association for Computing Machinery, New York, NY, USA, 487–499. doi:10.1145/2789168.2790100
- [44] H Zamani, A Abas, and MKM Amin. 2016. Eye tracking application on emotion analysis for marketing strategy. *Journal of Telecommunication, Electronic and Computer Engineering (JTEC)* 8, 11 (2016), 87–91.
- [45] Shichen Zhang, Pedram Kheirkhah Sangdeh, Hossein Pirayesh, Huacheng Zeng, Qiben Yan, and Kai Zeng. 2022. Authiot: A transferable wireless authentication scheme for iot devices without input interface. *IEEE Internet of Things Journal* 9, 22 (2022), 23072–23085.
- [46] Tianfang Zhang, Zhengkun Ye, Ahmed Tanvir Mahdad, Md Mojibur Rahman Redoy Akanda, Cong Shi, Yan Wang, Nitesh Saxena, and Yingying Chen. 2023. FaceReader: Unobtrusively Mining Vital Signs and Vital Sign Embedded Sensitive Info via AR/VR Motion Sensors. In *Proceedings of the 2023 ACM SIGSAC Conference on Computer and Communications Security*. Association for Computing Machinery, New York, NY, USA, 446–459. doi:10.1145/3576915.3623102
- [47] Xinze Zhang, Walid Brahim, Mingyang Fan, Jianhua Ma, Muxin Ma, and Alex Qi. 2023. Radar-Based Eyeblink Detection Under Various Conditions. In *Proceedings of the 2023 12th International Conference on Software and Computer Applications*. Association for Computing Machinery, New York, NY, USA, 177–183. doi:10.1145/3587828.3587855
- [48] Xiaotong Zhang, Zhenjiang Li, and Jin Zhang. 2022. Synthesized Millimeter-Waves for Human Motion Sensing. In *Proceedings of the 20th ACM Conference on Embedded Networked Sensor Systems*. Association for Computing Machinery, New York, NY, USA, 377–390. doi:10.1145/3560905.3568542
- [49] Xucong Zhang, Yusuke Sugano, Mario Fritz, and Andreas Bulling. 2015. Appearance-based gaze estimation in the wild. In *Proceedings of the IEEE conference on computer vision and pattern recognition*. IEEE, Piscataway, NJ, USA, 4511–4520. doi:10.1109/CVPR.2015.7299081
- [50] Xi Zhang, Yu Zhang, Zhenguo Shi, and Tao Gu. 2023. mmFER: Millimetre-wave Radar based Facial Expression Recognition for Multimedia IoT Applications. In *Proceedings of the 29th Annual International Conference on Mobile Computing and Networking*. Association for Computing Machinery, New York, NY, USA, 1–15. doi:10.1145/3570361.3592515
- [51] Wangjiang Zhu and Haoping Deng. 2017. Monocular free-head 3d gaze tracking with deep learning and geometry constraints. In *Proceedings of the IEEE International Conference on Computer Vision*. IEEE, Piscataway, NJ, USA, 3143–3152. doi:10.1109/ICCV.2017.341